

Frictional Contact Stress Analysis of Involute Spur Gear by Finite Element Method

by

Muhammad Farhan bin Dahan

Bachelor of Engineering (Hons)
(Mechanical Engineering)

September 2013

Universiti Teknologi PETRONAS
Bandar Seri Iskandar,
31750 Tronoh,
Perak Darul Ridzuan.

CERTIFICATION OF APPROVAL

Frictional Contact Stress Analysis of Involute Spur Gear by Using Finite Element Method

by

Muhammad Farhan bin Dahan

A project dissertation submitted to the
Mechanical Engineering Programme
Universiti Teknologi PETRONAS
in partial fulfilment of the requirement for the
BACHELOR OF ENGINEERING (Hons)
(MECHANICAL ENGINEERING)

Approved by,

(Dr. Saravanan Karuppanan)

UNIVERSITI TEKNOLOGI PETRONAS
TRONOH, PERAK
September 2013

CERTIFICATION OF ORIGINALITY

This is to certify that I am responsible for the work submitted in this project, that the original work is my own as specified in references and acknowledgements, and that the original work contained herein have not been undertaken or done by unspecified sources or persons.

MUHAMMAD FARHAN BIN DAHAN

ABSTRACT

Gear is one of the mechanical components that have been used since the early civilization such as Greek and China. One of the common types of gear is spur gear. Spur gear is used to transfer rotary motion between parallel shafts. The simplicity in its design is one of the advantages of the spur gear. However higher frictional force that is accumulated on the gear teeth will influence the spur gear performance and sometimes can cause failure such as pitting. Many previous papers elaborated more about the contact stress at the spur gear but few of them gave the detail about how friction affects the gear teeth. There is insufficient frictional effect data in the gear and thus should be regarded as important parameter. For this project, the author employed the analytical calculation and Finite Element Method. The analytical calculations have been computed by using Hertz Contact Stress Theory and AGMA Standard. Later, a 3D spur gear set has been modelled in CATIA and imported into ANSYS Workbench. The frictionless contact stress result has been validated with the both equations with a deviation of less than 10%. Frictional coefficient range from 0.1 until 0.3 was selected and the corresponding contact stress is directly proportional to frictional coefficient. Lastly, the author varied load applied and face width of the gear set under frictional influence. The relationship shows that the frictional contact stress is directly proportional to the face width and load.

ACKNOWLEDGEMENT

First and foremost, the author would like to express his highest gratitude to the supervisor, Dr Saravanan Karuppanan, for all the motivation, knowledge and advices that has been shared. The help received from him have led the author to a clear path in overcoming numerous obstacles when conducting this project.

The author would like to thank Mr Santosh Patil who has contributed in making this project successful. He has assisted and gave opinion to the author to complete this project.

Finally, the author would also like to express gratitude to Universiti Teknologi PETRONAS for providing research place in undertaking the project. Also personal thanks given to the family and friends whom have given constant support throughout.

TABLE OF CONTENT

CERTIFICATION OF APPROVAL	i
CERTIFICATION OF ORIGINALITY	ii
ABSTRACT	iii
ACKNOWLEDGEMENT	iv
LIST OF FIGURES	vii
LIST OF TABLES	ix
CHAPTER 1: INTRODUCTION	1
1.1 Background of Study	1
1.2 Problem Statement	4
1.3 Objective	4
1.4 Scope of Study	5
CHAPTER 2 LITERATURE REVIEW	6
CHAPTER 3 METHODOLOGY	11
3.1 Overview	11
3.2 Analytical Calculation	11
3.3 ANSYS Simulation (Frictionless)	14
3.4 ANSYS Simulation (Frictional)	18
3.5 Flowchart of the Procedure	19
CHAPTER 4 RESULT AND DISCUSSION	20
4.1 Analytical Calculation	20
4.2 Frictionless ANSYS Simulation	22

	4.3 Frictional ANSYS Simulation	23
CHAPTER 5	CONCLUSION AND RECOMMENDATION	29
REFERENCES		30
APPENDICES		32

LIST OF FIGURES

Figure 1.1: Primitive Gear	1
Figure 1.2: Spur Gear Nomenclature	2
Figure 1.3: Example of Spur Gears Application: Lathe Machine	3
Figure 1.4: Case Crushing	3
Figure 2.1: CONTA 174	9
Figure 3.1: Spur Gear Model	14
Figure 3.2: Contact Region Generation Menu	15
Figure 3.3: Frictionless Support Location	16
Figure 3.4: Moment Applied	16
Figure 3.5: Meshing of Spur Gear Set	17
Figure 3.6: Frictional Analysis Generation Menu	18
Figure 3.7: Flow Chart of the Project	19
Figure 4.1: Contact Stress vs. Load	21
Figure 4.2: Contact Stress vs. Face Width	22
Figure 4.3: Frictionless ANSYS Gear Analysis (3D)	23
Figure 4.4: Frictionless ANSYS Gear Analysis (Front Plane)	23
Figure 4.5: Contact Region of the Sphere	24
Figure 4.6: Contact Stress against Coefficient of Friction	25
Figure 4.7: Contact Stress under Influence of Friction	25
Figure 4.8: Contact Stress against Load under Influence of Friction	27
Figure 4.9: Contact Stress against Face Width under Influence of Friction	28

LIST OF TABLE

Table 2.1: Spur Gear Data	7
Table 3.1: Spur Gear Dimension	12
Table 3.2: Value of Parameters Used in AGMA Standard	13
Table 4.1: Contact Stress using Analytical Equation	20
Table 4.2: Result of Frictional Contact Stress	24
Table 4.3: Percentage Different between Frictional and Frictionless Contact Stress	27

CHAPTER 1

INTRODUCTION

1.1 Background of study

Gear is one of the mechanical components that play an important role for the humankind. Historically gear existed since 2600 BC in China for controlling the chariot. Some say the gear already been used 12000 years ago for the function of closing and opening of cave door. Aristotle recorded that during Greek Civilization gears being used in many applications. Painter and inventor Leonardo da Vinci also developed the tooth gear that served clocks in Cathedral. This kind of gear is still serving and is still in the good shape. The development of gear reached its peak during Industrial Revolution. During this time, the gears were being used for many applications such as water mills, irrigation devices, and power machine. This period has a major impact to the gear development and the gear technology. Since then gears have been advanced rapidly. Figure 1.1 shows the primitive gear that has been made up from wood.

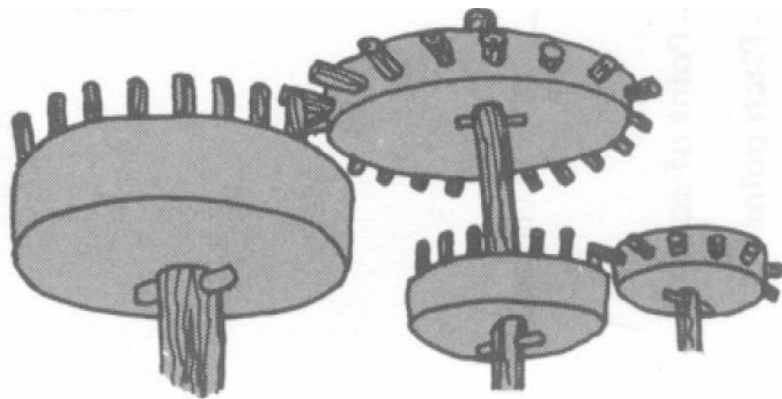


Figure 1.1: Primitive Gear

Gears can be defined as tooth mechanism member which transmit power or motion between two shafts by meshing without any slip. Gear set usually consists of two parts which are pinion and gear. The pinion serves as driver mechanism whereas gear acts as driving mechanism. There are many types of gears such as spur gear, helical gear and many more. Each type of gears has its own respective advantage. For the purpose of this report, the author will elaborate more about spur gear.

Spur gears are the most recognized and common type of gear. Spur gears have their teeth parallel to the axis and are used exclusively to transmit rotary motion between two parallel shafts, while maintaining uniform speed and torque. They have the highest efficiency and excellent precision rating. The involute tooth form being the simplest to generate, permits high manufacturing tolerances to be attained.

The advantages of spur gear come from their simplicity in design, cost to manufacture and maintenance, and the absence of end thrust. They are used in high speed and high load applications. They impose radial loads on the bearings. The spur gears are used in wide applications right from simple clocks, household gadgets, motor cycles, automobiles, and railways to aircrafts. However, this type of gear is noisy and because of that, the gear is not suitable to be used in the car system. The nomenclature of spur gears and the example of the spur gears application is shown in Figure 1.2 and Figure 1.3, respectively.

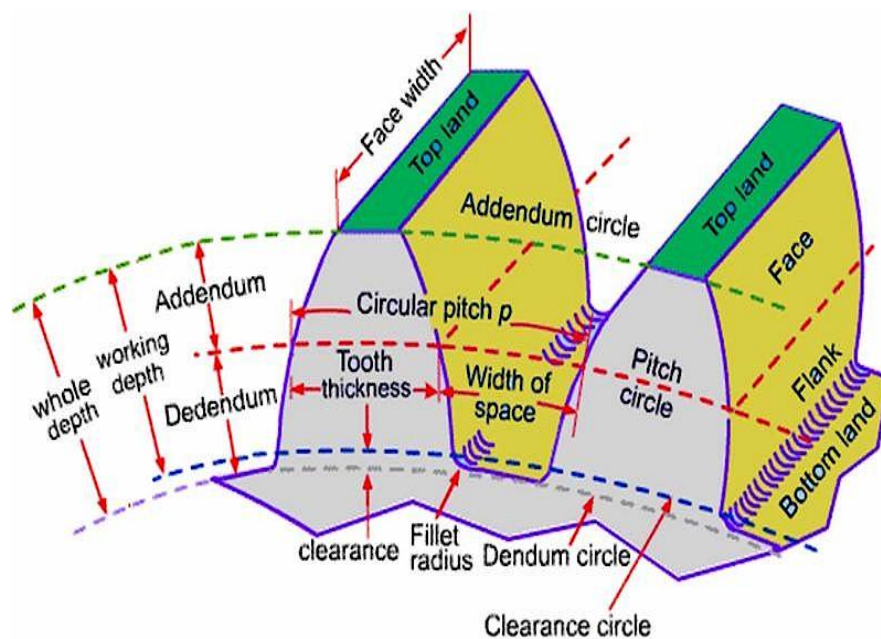


Figure 1.2: Spur Gear Nomenclature [21]



Figure 1.3: Example of Spur Gears Application: Lathe Machine

Apart from becoming the reliable component to transfer mechanical power or output, gears also sometimes develop failure that prevents them from performing their duty efficiently. These failures are due to many factors such as improper method of maintenance, the fatigue and sometimes caused during the manufacturing of the gears itself. There are many types of the gear failures such as gear scuffing, pitting, case crushing and many more. One of the failures, pitting, is because of the repetitions of the high contact stress occurring on a gear tooth surface while a pair of teeth is transmitting power. Another failure which is the case crushing is also triggered by having high contact stress. In the case crushing, the crack will appear on the contact surface of the gear. Figure 1.4 illustrates the case crushing.

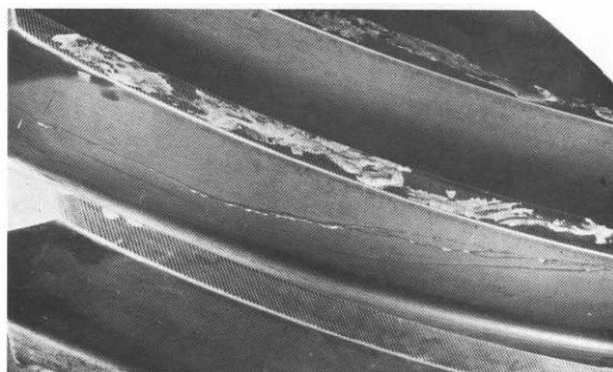


Figure 1.4: Case Crushing

When the case is too thin and the gear teeth are too low in hardness, the contact stress will break through the case, damaging the core. One of the reasons that cause the higher contact stress is friction. Friction will develop when two contact surfaces are moving. Frictional force will cause loss to the applied load. Friction also generates heat to the gear surfaces. Excessive heat generation can disturb the gear to function accordingly and this heat also will reduce the gear power.

In order to analyse the behaviour of the contact stress, the stress analysis need to be done. Stress analysis is the study on the stress behaviour of a structure. There are different types of stress but for this project, the author will focus on the contact stress. In this project the structure is spur gear itself. The analysis is conducted through several ways such as analytical method and numerical method. The numerical method chosen for this project is the Finite Element Method. Generally Finite Element Method will discretize the structure into many small elements. This is useful when complex problems are analysed.

1.2 Problem Statement

Spur gear is a variant of the gear technologies which is worth to investigate due to its function. Although there are already many papers or research regarding the stress analysis of the spur gear, not much of them are discussing the pattern of contact stress that include the friction. This brings the author the opportunity to describe and elaborate the role of friction in the gear and simulate them by using Finite Element Method to find the significant relationship between the friction and contact stress.

1.3 Objective

The objective of this project is to find the relationship between friction and contact stress in spur gear. This objective can be divided into three parts which are:

- 1) Utilization of Hertz equation to solve the contact stress
- 2) Utilization of 3D FEM modelling to simulate the contact stress and to validate the result with the analytical equation.
- 3) Utilization of 3D FEM modelling to simulate the contact stress of the spur gear under the influence of friction.

1.4 Scope of Study

The scope of study was to determine the contact stresses using the FEM method and to compare with the analytical calculation using Hertz and AGMA Standard. The FEM simulation will be completed by using ANSYS Workbench 14.5. The modelling of the spur gear will be carried out by CATIA. A pair of gear that consists of pinion and gear will be selected. The teeth for the pinion are 22 while for the gear is 55. 3D FEM analysis has been selected. The author selected steel as the gear's material. The FEM model will be validated by the Hertz and AGMA Standard. After that, the frictional contact stress simulation will be carried out. This simulation will be done by using frictional coefficient range from 0.1 until 0.3.

CHAPTER 2

LITERATURE REVIEW

In mechanical engineering, contact stress can be defined as the stress within mating parts. Every mating part that has contact will experience deformation. Basically this deformation has been caused by stress. According to Hertz theory, the contact for two sphere is a point and for the cylinder is the line. However, since this will result in infinite value of pressure between two curved bodies, a small contact area is established. The contact area is known as Hertz Contact Stress area. The assumption that has been used is the contact between two gears will be treat as contact between two spheres [1]. Thus the equation is given by:

$$P_{max} = \frac{3F}{2A^2} \quad (1)$$

where:

A = radius of contact area

F = load or force applied on the contact area

P_{max} = maximum pressure at the contact area

With the availability of modern technology, the reliable method for analysing the contact stress is available. This development gave opportunity for researchers to analyse and solve more complex contact problem. Thus, this ensures that the result can be validated. In 2003, Sorin Canacau in his paper studied the difference between the 2D and 3D approach in contact stress analysis [2]. The 3D approach is applied to investigate whether the fillet stress can be ignored or not. For his research, the code for finite element analysis used was MSC-Nastran 2.1. Table 2.1 shows the data for spur gear used in his paper.

Table 2.1: Spur Gear Data

Number of teeth, Z_1/Z_2		17/31
Centre distance, a	[mm]	120
Pressure angle, α_n	[deg]	20
Module, m	[mm]	5
Diametral pitch, p_n	[mm]	15.7080
Working face width, b	[mm]	40
Young Modulus, E	[N/mm ²]	2.07×10^5
Poisson's ratio, ν	-	0.32

Both of the approach used the involute spur gear. For the 2D model, the contact is assumed to be frictionless and the dynamic effects are not taken into account. In 3D model, the only part concerned is the part that has sensitive effect from the load applied. The sensitive part is the face width surface. From this paper three conclusion can be made. First of all the stress distribution in front plane of the 3D model is the same with the 2D model but with smaller variation around 10%-15%. The stress distribution along face width has the same shape as the load distributions for the same surface. Lastly the stress increase under non uniform contact in meshing process.

In 2009, Ali Raad Hassan developed a programme to plot a pair of teeth in contact. He also found that the stress from calculation and also stress from Finite Element Method is quite similar. The contact stress from the calculation is 587 MPa while the stress from the Finite Element Method is 595 MPa [3]. The stress analysis has been done by using ANSYS Mechanical APDL software. This shows that Finite Element Method can be used to validate any calculation and the software is reliable. Among the parameters that have been considered for his research were contact ratio, approach angle, recess angle, contact and length of contact. For this research, the changing parameter was contact position. This position is determined by the angle of the rotation. The angular interval used was 3° which mean that the contact angle is increased 3° for every section. Different angle of rotation gave the different value of the contact stress. From the analysis, high value contact stress can be seen at the beginning of the contact and decrease gradually until the single tooth contact.

Shinde *et al.* in 2011 suggested that stress distribution in Finite Element Method gave reliable comparison with the theoretical result [4]. There were three main objectives of this paper. The first one was to determine the bending stresses by using ANSYS and to compare the results with analytical result. The second objective was to predict the effect of gear bending stresses by using three dimensional model and to compare the results with the Lewis equation. Last objective was to compare the accuracy of the obtained result by varying mesh density. At the first stage all the theoretical calculations have been calculated by using Lewis Theory. Then, a gear was created by using Computer Aided Design software call PRO-E. Next, the model has been imported into the ANSYS Mechanical APDL and the meshing process will be done. The accuracy of the analysis is around 89% until 99% depending on the element size used. If the element size used is large the accuracy is decreased. From this paper, the conclusion that can be made was ANSYS software is capable to solve root bending stress and contact stress problem.

Gurumani and Shanmugam in 2011 developed a model of crowned spur gears. The objective of this paper is to investigate the performance between involute crowned gear teeth and normal circular spur gear teeth. In their paper, the design parameters that have been used were the centre distance between gear, module and number of gear teeth. All of these parameters have been analysed by using Finite Element Method. Both of them suggested that the contact area of involute spur gear is slightly less than the normal circular crowned spur gear. Therefore, the contact stress of circular crowned spur gear is higher than the involute crowned spur gear [5].

Usually the gear tooth will be covered. However if the gear tooth is wrongly covered, the efficiency of gear will be decreased. Martins *et al.* discovered that wrong coating material will increase frictional coefficient between the teeth. Higher hardness, low friction coefficient with a good adhesion is what the gears needed [6]. Low friction coating is one of the reasons of gear scuffing.

Friction is a daily process that affects several occurrences such as wear and thermal. Frictional phenomena will transformed the mechanical energy into heat. The maximum temperature that occurs on the contact surface can have an important influence on the behaviour of the contacting elements. In 2011, Stefancu *et al.* used the CONTA 174 to model frictional contact [7]. The CONTA 174 is shown in Figure 2.1.

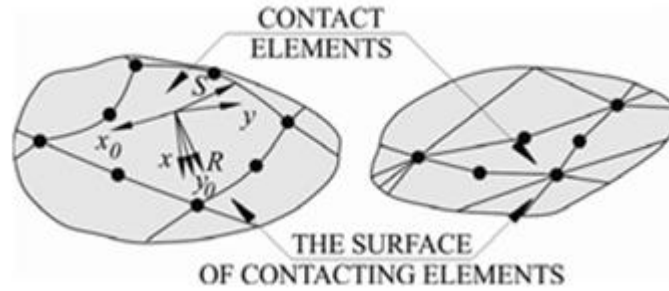


Figure 2.1: CONTA 174

The maximum values of the frictional stresses, shear stresses and normal stresses are proportional to the frictional coefficient and normal force. However, Stefancu concluded that experimental approach should also be considered to confirm the result of the analysis. This is because there is no model that can accurately describe all of the attributes stated above.

In 2013, Hwang *et al.* analysed the contact for a pair of mating gear [8]. From their research, they were convinced that the change in the load is one of the reasons of surface pitting. They utilized two-dimensional finite element model to calculate the contact stress. At first, they found the highest and lowest point of single tooth contact in spur gears. From there they calculated the spur gear's roll angle which was 27.4° . After that, the finite element model was constructed and the contact stress was found by using Abaqus 6.9. The results showed that the maximum stress was generated at the contact point and propagated along diagonally.

As stated earlier, there is no much data or research paper regarding the frictional contact stress in spur gear. The closest one was by Vijarangan and Ganesan in 1994. In their paper, the static friction coefficient has been varied from 0 until 0.3 [9]. The static contact stress was increased about 5%. The contact stress magnitude decreased to half the value at the depth of 0.5 mm contact surface. This discovery gave a roughly idea about the depth of hardness required. The maximum contact stress was located on the pitch point.

Recently in 2012, Koisha and Doshi investigated the influence of friction on contact stress for small power transmission planetary gear box [10]. Random friction coefficients from 0.05 until 0.15 have been varied. The research has been done by using

ANSYS Workbench. The frictionless contact stress simulation has been compared against the Standard ISO 6336 Part 2. The variation was only about 2%. Later, the graph of contact stress against friction coefficient has been plotted. The pattern of the contact stress is linear and its slope is lower due to low power transmission of the gear box.

CHAPTER 3

METHODOLOGY

3.1 Overview

This chapter contains four sections (excluding this section) to explain the methodology that has been carried out by the author to complete this project. The first section will be dealing with the analytical calculation. The second section will be focusing on the ANSYS simulation. The objective of the first section is to calculate the analytical contact stress value. To achieve this objective, the author will utilize two equations which are Hertz Contact Stress Theory (Equation 2) and AGMA Standard (Equation 3). The second part of this chapter will be elaboration of ANSYS simulation procedure that has been carried out by the author. This section includes modelling and simulation process.

3.2 Analytical Calculation

For the purpose of this project, the analytical value of the contact stress needs to be evaluated. Values obtained from analytical calculation gave reader an understanding on the magnitude of the contact stress that has been exerted by the gear set. In the real world or industry, this value serves as the indication whether the gear design is safe or not. The most important attributes in analytical calculation are the equation and parameter. Below is the complete procedure for the analytical calculation.

1. A spur gear set will be chosen.

The first thing that has been carried out by the author was choosing a spur gear set. The gear set primarily consists of pinion and gear. The pinion will act as the master while the gear will act as slave. Therefore, the moment will be applied on the pinion. From the moment applied, the gear will rotate accordingly. Gear mesh will developed uniform rotary motion between them. In the analytical calculation, the parameter of the gear will be inserted in the analytical equation to find the contact stress. Table 3.1 shows the information of the selected spur gear in terms of dimension parameter.

Table 3.1: Spur Gear Dimension

Parameter	Pinion	Gear
Pressure Angle	20 °	
Module	8 mm	
Pitch Diameter	176 mm	440 mm
Base Diameter	165.39 mm	413.46 mm
Number of Teeth	22	55
Face Width	120 mm	

- The theoretical contact stress value will be evaluated.

The contact stress of the gear set will be determined by using Hertz Theory equation and also AGMA Standard. All of the dimension parameters will be inserted into these equations. For the modulus of elasticity and Poisson's ratio, the author assumed that both of the gear material is steel. This gave the value of 200 GPa and 0.3, respectively [8].

The Hertz Theory Contact Stress equation is:

$$\sigma = \sqrt{\frac{W \left(1 + \frac{r_{p1}}{r_{p2}}\right)}{r_{p1} F \pi \left[\frac{(1-\nu_1^2)}{E_1} + \frac{(1-\nu_2^2)}{E_2} \right] \sin \phi}} \quad (2)$$

where:

W = load

r_{p1} = pitch radius of the pinion

r_{p2} = pitch radius of the gear

F = face width

ν_1 and ν_2 = Poisson's ratio for the pinion and gear which is 0.3

E_1 and E_2 = Modulus of elasticity of the steel which is 200 GPa

ϕ = pressure angle

For the AGMA standard, the equation is:

$$\sigma = Z_e \sqrt{F_T K_0 K_V K_S \frac{K_H}{2 r_1 w Z_1}} \quad (3)$$

where:

Z_e = coefficient factor

F_T = Load

K_0 = Overload factor

K_V = dynamic factor

K_S = size factor

K_H = load distribution factor

r_1 = pinion's pitch radius

W = face width

Z_1 = geometry factor for pitting resistance

Table 3.2: Values of Parameters Used in AGMA Standard

Parameter	Value
Z_e	191 MPa
F_t	9000 N
K_0	1.0
K_V	1.0
K_S	1.0
K_H	1.0
r_1	88 mm
W	120 mm
Z_1	0.115

The values of the parameters related in AGMA Standard are defined in the Table 3.2. The value of the coefficient factor is from Table 11-18 AGMA Elastic Coefficient [8]. This value is a common value for a gear set that is made up from steel. The overload factor was taken from the operating characteristic of driving machine. The author assumed that the gear is in uniform operating machine such as in electric motor. The dynamic factor value was taken from Dynamic Factor curve. It was assumed that after manufacturing process, the gear set was in the good condition and does not have defect. The size factor value is 1 because of the normal teeth size. Besides, the load was assumed to be distributed evenly on the face width. Therefore, this condition gave the

load distribution factor of 1. The value of the geometry factor for pitting resistance was selected because of number of teeth of gear and pinion [12].

3.3. ANSYS Simulation (Frictionless)

Finite Element Method needs to be validated to ensure its reliability. In order to complete the validation process, Finite Element Method (FEM) results were compared with analytical results. The difference between FEM and analytical result must be less than 10 %. Finite element method is one of the modern techniques used to perform stress analysis. The basic concept of this method is replacing the complicated problem with a simpler problem. The solution region is divided into small interconnected finite elements. This method saves time compared to the conventional method. Historically this method is developed by NASA as a tool to analyse their space ship. Finite element method has two types of analysis which are 2D analysis and 3D analysis. In this project, the author will use the 3D analysis. The software that will be used in this project is ANSYS Workbench 14.5. The reason why the author has chosen this software was because of its compatibility with 3D modelling. Below is the complete procedure of this section.

1. The spur gear set will be modelled.

After the completion of analytical calculation, the finite element will be carried out. 3D spur gear will be modelled by using CATIA and then be imported to ANSYS. The 3D model is shown in Figure 3.1.

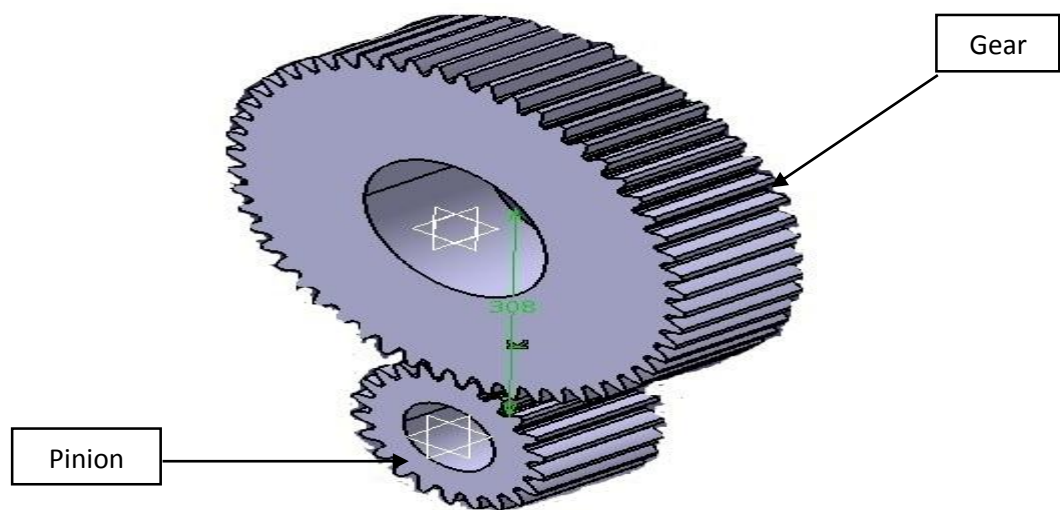


Figure 3.1: Spur Gear Model

2. The 3D Gear model will be imported into ANSYS Workbench 14.5.

FEM will be using static structural analysis in ANSYS. Before that, the 3D Gear model needs to be saved in the IGES mode. In IGES mode, ANSYS can read other software's file. Next, the FEM analysis is set up into 3D analysis.

3. The contact region will be specified.

After importing the gear set, the contact type of the spur gear will be specified. In the ANSYS Workbench, the contact types available are bonded, separation, frictionless, rough and frictional. The contact type chosen was frictionless to validate the gear model and frictional to simulate the spur gear set under the influence of friction. Figure 3.2 shows the contact region generation menu in the ANSYS Workbench.

Definition	
Type	Frictionless
Scope Mode	Automatic
Behavior	Symmetric
Trim Contact	Program Controlled
Trim Tolerance	1.9691 mm
Suppressed	No
Advanced	
Formulation	Augmented Lagrange
Detection Method	Program Controlled
Penetration Tolerance	Program Controlled
Interface Treatment	Adjust to Touch
Normal Stiffness	Program Controlled
Update Stiffness	Program Controlled

Figure 3.2: Contact Region Generation Menu

4. Boundary condition will be specified.

In the analysis section, the boundary condition will be defined. Boundary condition is defined as a condition that is required to be satisfied, at all or part of the boundary of a region in which a set of differential conditions are to be solved. In the simple words, boundary conditions specify the location of support and load. It is also referred to the external load in the boundary structure. For this project, the frictionless supports were attached to both of the gear and the pinion shaft. This type of support is used to allow rotation at the Z-axis. The reason why the author has chosen this support is to make sure the bodies will fix and only the rotational motion at the Z-axis is allow. Figure 3.3 shows the frictionless support location.

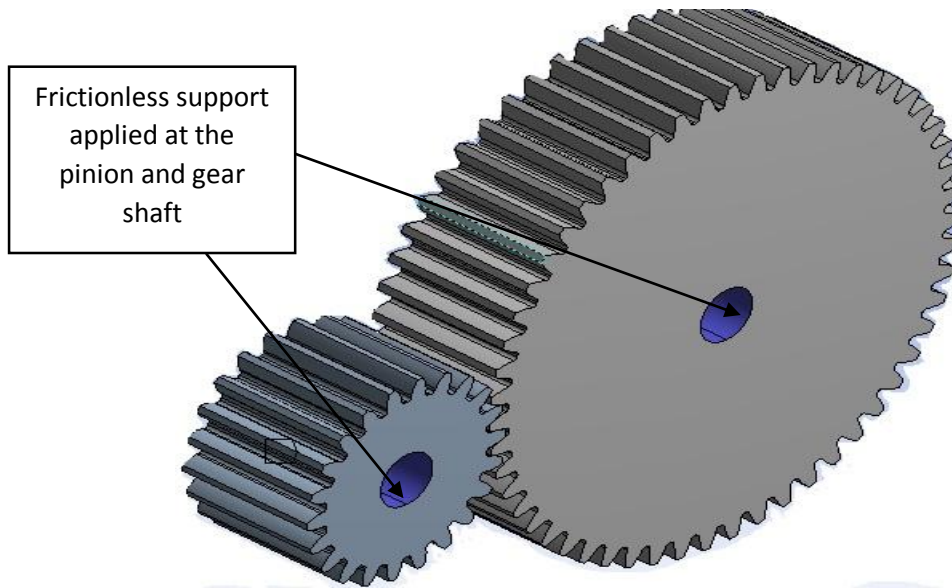


Figure 3.3: Frictionless Support Location

As stated earlier, the author treats pinion as the driver. Therefore moment will be applied at the pinion shaft. The moment value is 794820 N.mm. According to Hwang *et al.* the moment applied is the product of the pitch radius and tangential load [8]. The rotation direction was in the clockwise direction. Figure 3.4 will illustrate the location of moment applied.

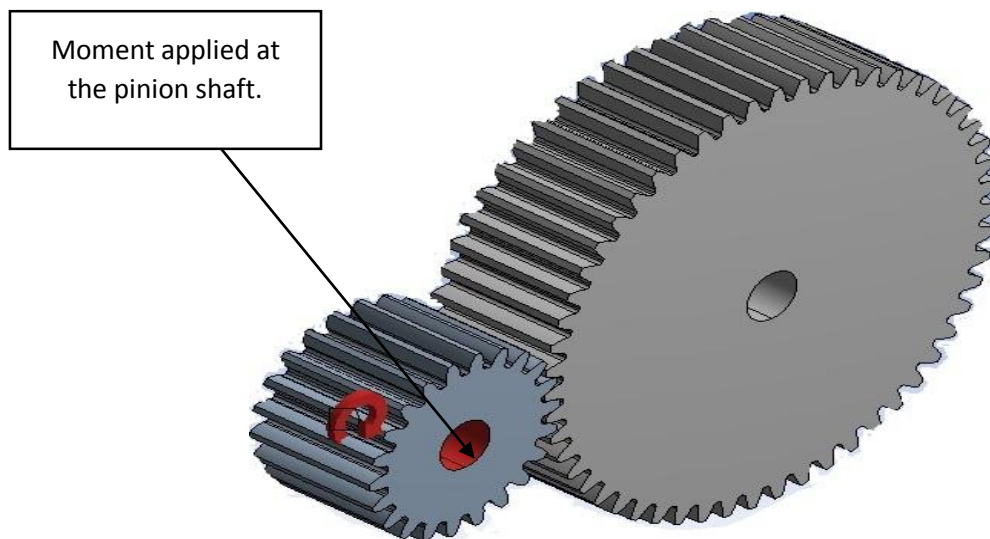


Figure 3.4: Moment Applied

5. Suitable meshing was generated.

Meshing is representation for finite element set used for computational and modelling and should be generate correctly to ensure the result obtained is reliable. Meshing should be fine at the area of contact region. It is not suitable to use the fine meshing in all available body. This is due of time constraint and the performance of computer. The author used Solid 187 element type. This element type is common choice for the solid model. The meshing type that has been selected was tetrahedron. The number of element was 105741 and the number of nodes was 175376. There are six degrees of freedom involved which were displacement at X, Y and Z and also rotation at X, Y and Z axis. There was 1306 number of contact. The size of the meshing was 0.254 mm. This was the optimum size considering the factor such as time constraint and computer performance. It is not practical to use the fine meshing in the whole body. This is due to time constraint and the performance of the computer. Figure 3.5 illustrates the meshing of the spur gear set.

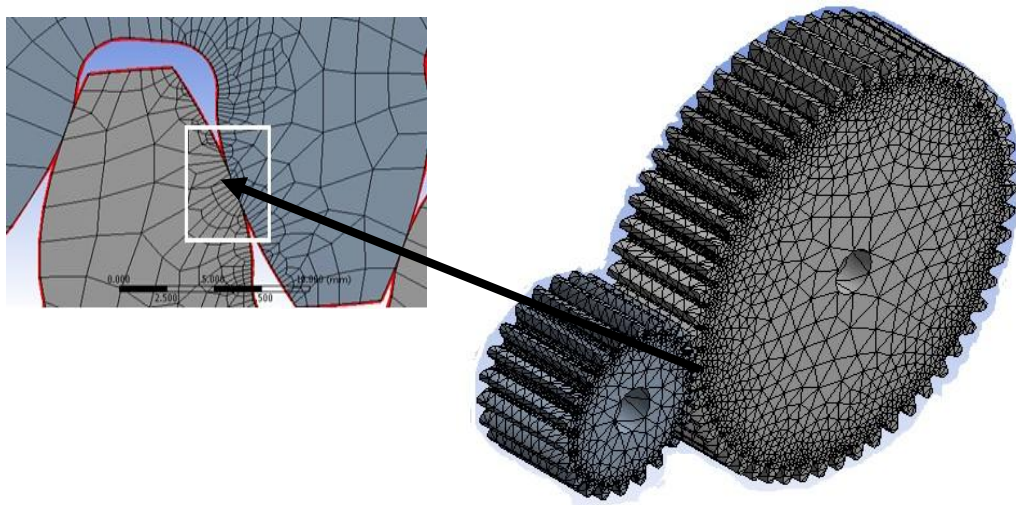


Figure 3.5: Meshing of Spur Gear Set

6. The model was solved and the contact stress will be recorded.
7. The frictionless contact stress value taken from simulation will be compared with the analytical values.

3.4 ANSYS Simulation (Frictional)

1. The contact type was changed into frictional contact.

The frictional analysis will be carried out by changing the contact region into frictional. Then, frictional coefficient between 0.1 until 0.3 will be varied. All of the procedure mentioned above was maintained. Figure 3.6 shows the option for the frictional analysis in the ANSYS Workbench.

Definition	
Type	Frictional
<input type="checkbox"/> Friction Coefficient	0.1
Scope Mode	Manual
Behavior	Symmetric
Trim Contact	Program Controlled
Suppressed	No
Advanced	
Formulation	Augmented Lagrange
Detection Method	Program Controlled
Penetration Tolerance	Program Controlled
Elastic Slip Tolerance	Program Controlled
Interface Treatment	Adjust to Touch

Figure 3.6: Frictional Analysis Generation Menu

2. The model was solved and the contact stress result will be recorded. The contact stress against frictional coefficient will be established.

Later, by using the same gear set model and the frictional contact type, the load will be varied. The objective of this procedure is to find the relationship between contact stress and load under the influence of friction. Later, the gear set model will be modified by changing the face width and the gear set will be simulated again. The reason is to find the relationship between contact stresses and face width under the influence of friction.

3.5 Flowchart of the Procedure

Figure 3.7 shows the flowchart of the project. This flow chart served as the guideline to help reader understands the methodology that has been carried out by the author in the simple manner. The completed Final Year Project 1 and Final Year Project 2 Gantt chart can be referred to Appendix 3-1 and 3-2.

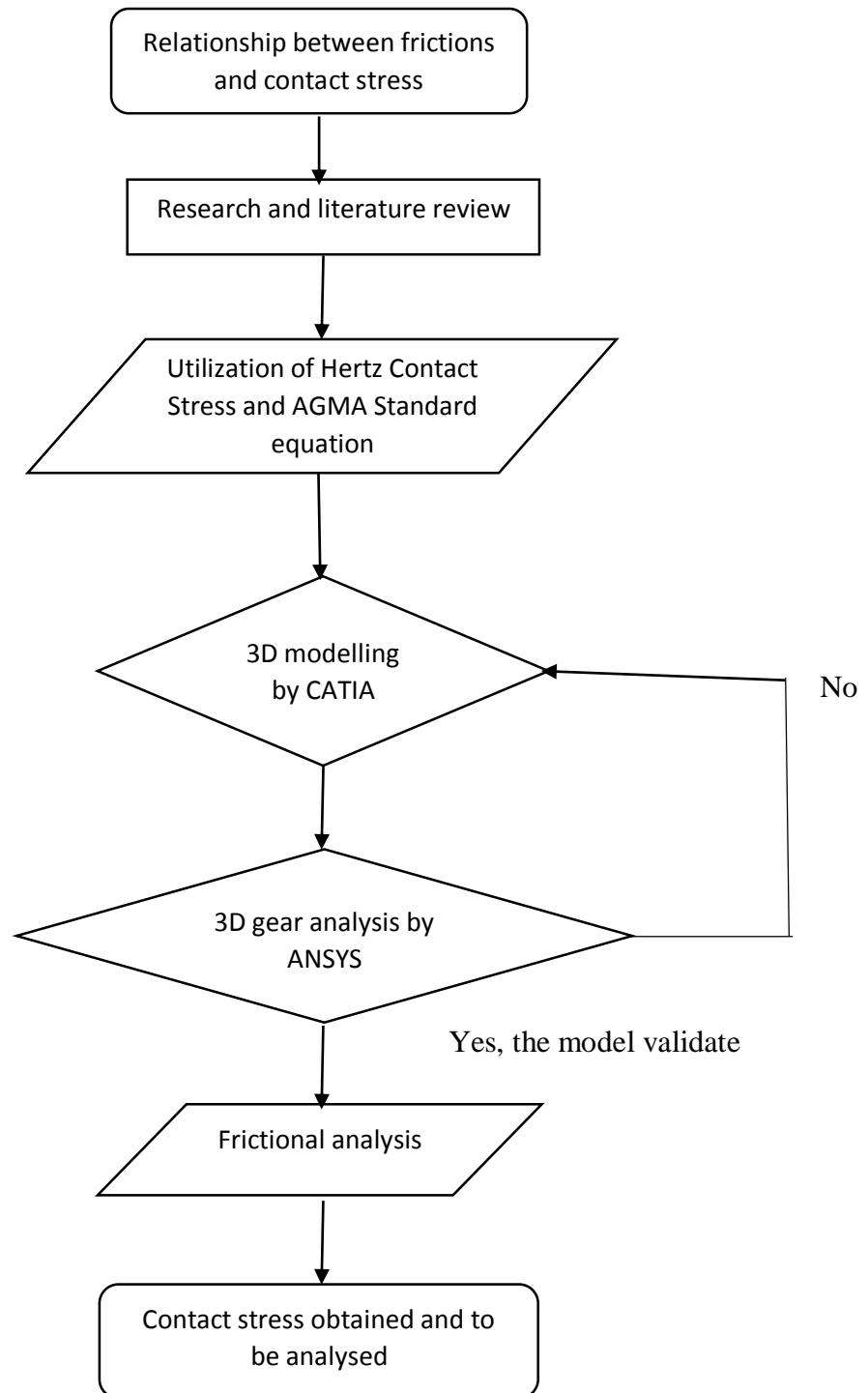


Figure 3.7: Flow Chart of the Project

CHAPTER 4

RESULTS AND DISCUSSION

4.1 Analytical Calculation

The author has completed the analytical calculation by using both Hertz Theory and AGMA Standard. The detailed of the analytical calculations involved for this study have been stated in Chapter 3. By using those equations, the author managed to solve and acquired the numerical value of the contact stress. The contact stress for Hertz Theory and AGMA Standard are shown in Table 4.1.

Table 4.1: Contact Stress Using Analytical Equations

Hertz Theory	AGMA Standard
350 MPa	360 MPa

The above information shows that the contact stress magnitude between both of the analytical equations is quite similar. This is because the deviation percentage between them was only 2.85 %. After carrying out these calculations, the next step was to model and perform static structural analysis in ANSYS Workbench. However to get a better understanding of the contact stress behaviour, the author decided to plot the graph of selected parameters against the contact stress. The selected parameters were load and face width. This action was done by varying these parameters value and substituting them in those equations. The other remaining values are set to be constant. Then, the contact stresses obtained were recorded. Later, after the frictionless and frictional analysis have been done by using ANSYS Workbench, the results were compared. Figure 4.1 shows the graph between loads applied and contact stress.

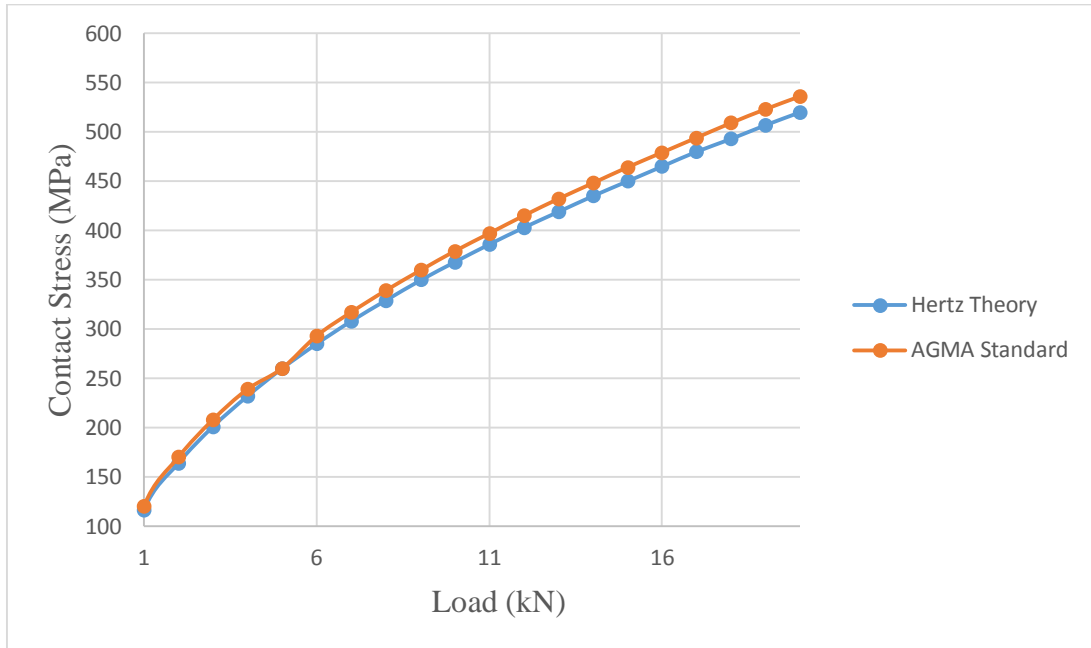


Figure 4.1: Contact Stress vs. Load

The relationship shows that the contact stress is directly proportional to the varied load. The load range is from 1 kN to 20 kN. The highest contact stress was obtained when the highest load was used. Initially the contact stresses between two analytical equations were quite similar. At this moment, the contact stress increased at higher rate when the load applied was increased. However when 6 kN load was applied, the graph line between them started to break. AGMA Standard has greater contact stress value compared with the Hertz Contact Stress Theory. At this applied load, the contact stress increment reduced gradually as the load was further increased. The contact stress produce must not exceed the ultimate tensile strength, which is in this case is 623 MPa. If the value exceed, the gear failure will be occurred. After obtaining this relationship, the works are continued by finding the relationship between face width and contact stress. Figure 4.2 shows the graph of contact stress against face width.

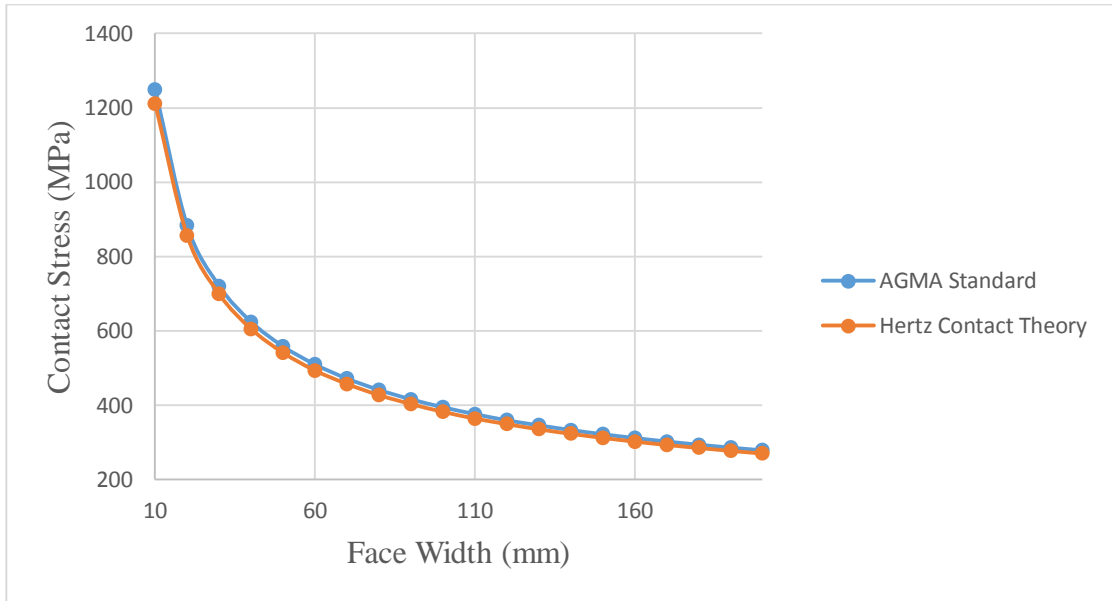


Figure 4.2: Contact Stress vs. Face Width

The graph shows the influence of face width against the stress. The face width is varied from 10 mm to 200 mm. The interval between the face widths is 10 mm. Then, the values of the contact stresses were obtained. The relationship suggested that as the face width increases, the contact stress decreases. The depreciation value of every contact stress interval is being calculated. From the graph, the highest contact stress took place at the lowest face width. Here, at the first face width interval, the difference between the contact stresses is 355 MPa for Hertz Contact Theory and 366 MPa for AGMA Standard. The decreasing percentage is around 30 %. Both of the values show that the spur gear has exceeded the tensile strength and exposed to the crack. For the next interval, the decreasing percentage is around 19 % and lastly the contact stresses percentage is only 2.4 %. The graph also confirmed the role of the face width which is to distribute the load applied evenly to the spur gear. From the values obtained, the author suggested that the minimum face width for this spur gear set is above 40 mm.

4.2 Frictionless ANSYS Simulation

After completing the analytical calculation, the simulation of the spur gear set in ANSYS Workbench was carried out. The simulation began with the frictionless analysis. The objective of the simulation was to determine whether the spur gear set was correctly modelled. In this simulation the contact stress obtained was 379.52 MPa. When this value was compared with the Hertz Theory and AGMA Standard the deviation was 8.4 % and 5.4 %, respectively. This deviation is considered reasonable

and acceptable as the limit of percentage deviation is not exceeding 10 %. This means that the spur gear set is modelled correctly and ANSYS Workbench results can be used. Figure 4.3 and Figure 4.4 show the frictionless ANSYS gear analysis in 3D and also at front plane, respectively.

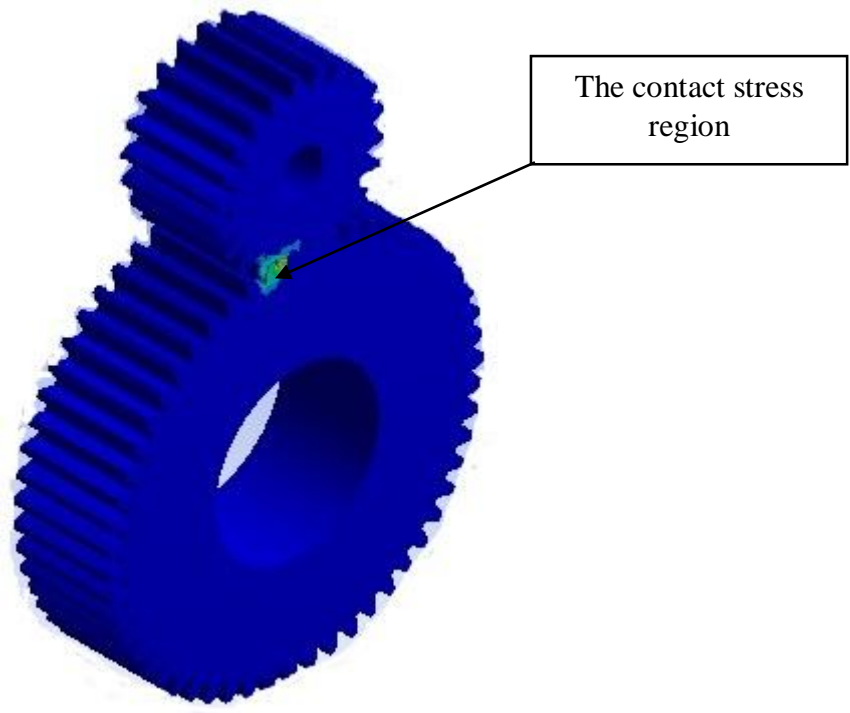


Figure 4.3: Frictionless ANSYS Gear Analysis (3D)

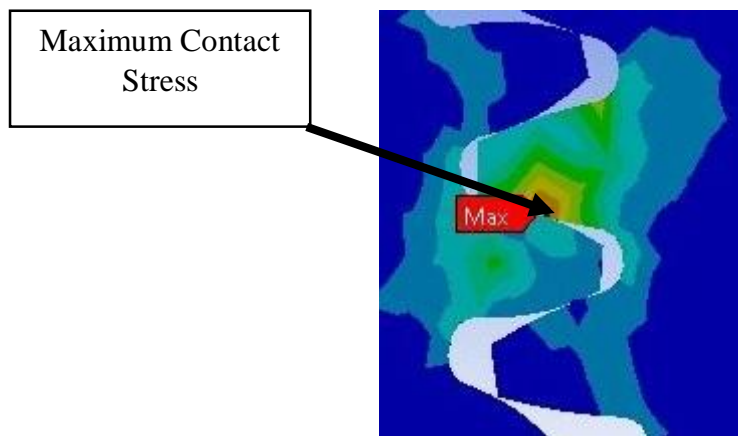


Figure 4.4: Frictionless ANSYS Gear Analysis (Front Plane)

In this simulation, the maximum contact stress value lies on the contact surface between two teeth. This trend is consistent with the Hertz Theory. This is because the contact stress location is within the Hertz Theory contact area of the sphere as in Figure 4.5. This location is the most affected location and need to be taken care properly.

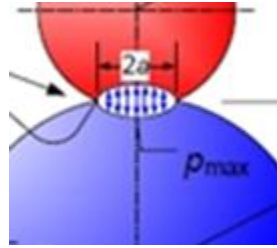


Figure 4.5: Contact Region of the Sphere [1]

4.3 Frictional ANSYS Simulation

After completing the analytical calculation and frictionless simulation, the next step was to find the relationship between the friction and contact stress. For the frictional analysis, the coefficient of friction that has been chosen was from the range of 0.1 until 0.3. This range was chosen to give a basic understanding about the behaviour of the contact stress that has been influenced by friction. Three graphs are evaluated from the simulation. They were contact stress against coefficient of friction, contact stress against load under the influence of friction and contact stress against face width under the influence of friction. Generally under the influence of friction the contact stresses were increased. This is consistent with the fundamental theory. The main concerning factor to be considered is how much the increment of the contact stress. This relationship has been generated by ANSYS Workbench. Table 4.2 shows the frictional contact stress for respective coefficient of friction. The moment used for this simulation was 794820 N.mm and the face width used was 120 mm.

Table 4.2: Result of Frictional Contact Stress

Coefficient of Friction	Contact Stress (MPa)
0.000	379.52
0.025	381.60
0.050	383.72
0.075	384.81
0.100	386.19
0.125	385.95
0.150	386.74
0.175	388.26
0.200	393.13
0.225	394.22
0.250	396.70
0.275	399.19
0.300	401.58

The table shows that the difference between frictionless contact stress and contact stress for friction coefficient of 0.3 is 21.66 MPa. This is equal to 5.8 % of increment. Figure 4.5 shows the relationship between contact stress and coefficient of friction. This pattern line was plotted by using Microsoft Excel.

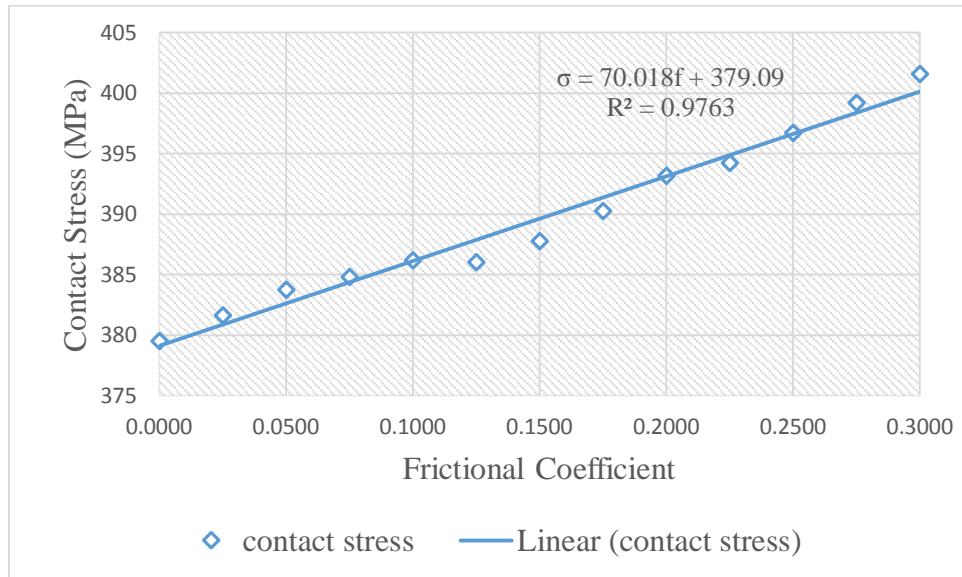


Figure 4.6: Contact Stress against Coefficient of Friction

The slope of this graph has been determined and has value of 70.018. Therefore, the straight line equation is:

$$\sigma = 70.018f + 379.09 \quad (4)$$

where:

σ = contact stress

f = frictional coefficient

This equation gave an idea about how to find the frictional contact stress for this type of gear. However the geometry data must be the same as data that has been elaborated in Chapter 3. This is because different parameter give different contact stress. For example a small pitch radius will experience more contact stress than the bigger pitch radius.

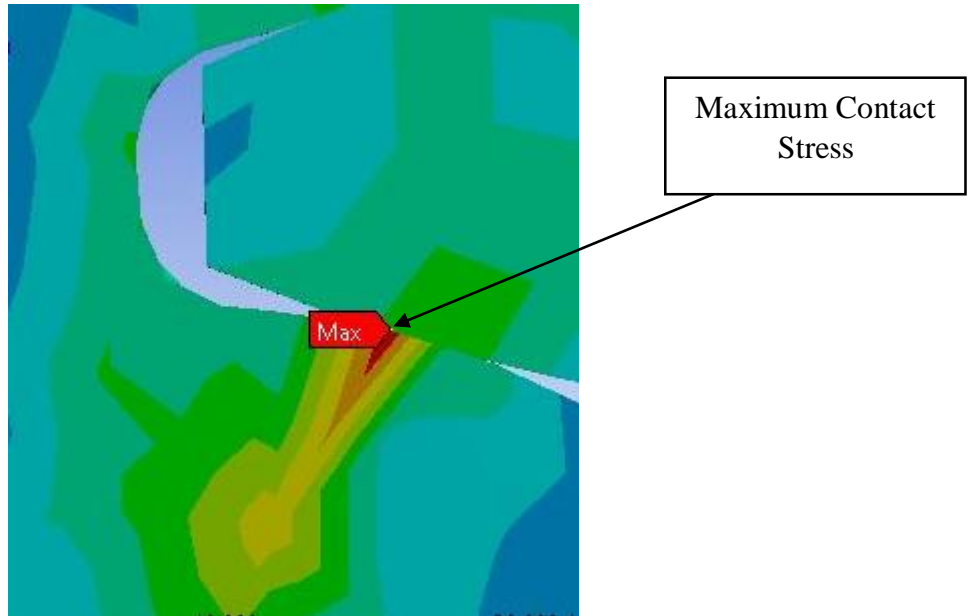


Figure 4.7: Contact Stress under the Influence of Friction

From Figure 4.7, the maximum contact stress is developed at the pitch point between two teeth. This location is consistent with the maximum frictionless contact stress location. The location is also consistent with the previous research made by Vijarangan and Ganesan [9]. Both of them concluded that the maximum contact stress will occur at that location. This happened because at this point, the involute curve is at the outermost layer. Both of the teeth will contact each other more frequently compared to the other part of the gear tooth.

Finally, the relationship between load and contact stress under the influence of friction was found. The load was varied and the frictional contact stress was obtained. Under the influence of friction the contact stress was increased. At the beginning of the analysis the load used was 1000 N. The frictionless contact stress by using this amount of load is 62.88 MPa. Then, the contact stresses under the influence of frictional coefficient at this magnitude of load are 64.02 MPa, 65.08 MPa and 66.58 MPa. Notice that these values of contact stress are close with each other. Their percentage of increment is about in the range of 1.6 % until 2.3 %. Full result of this analysis can be referred in Appendix 4-1.

The percentage of differences among the contact stresses at every frictional coefficient compare to the frictionless contact stress is increases. The percentage of differences between each of the frictional contact stress compare with the frictionless

case is illustrated in the Table 4.3. The pattern of the contact stress is illustrated in the Figure 4.8.

Table 4.3: Percentage Different between Frictional and Frictionless Contact Stress

Frictional Coefficient	Frictional Coefficient of 0.1	Frictional Coefficient of 0.2	Frictional Coefficient of 0.3
Percentage (%)	1.89	3.66	5.81

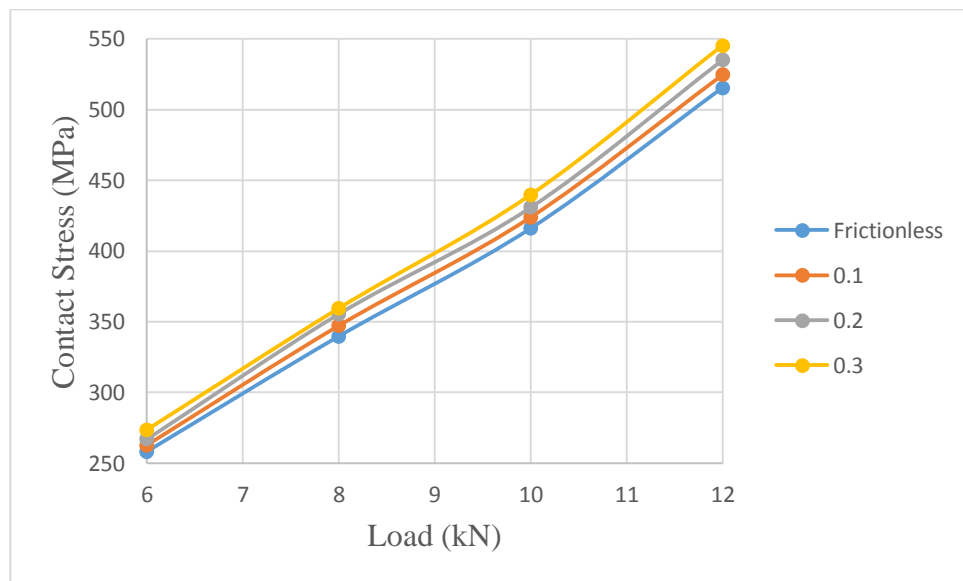


Figure 4.8: Contact Stress against Load under the Influence of Friction

The graph shows common result when the load increases. The range of the load was chosen from 6 kN until 10 kN. After varying the load to find the contact stresses under the influence of friction, the relationship between contact stress and face width under the influence of friction was found. This is carried out by modifying 4 more gear set that has different face width. The face width chosen were 80 mm, 100 mm, 140 mm, 160 mm and 180 mm. Apart from different face width, all of other procedure remains the same. Figure 4.9 shows the contact stress against face width under the influenced of friction.

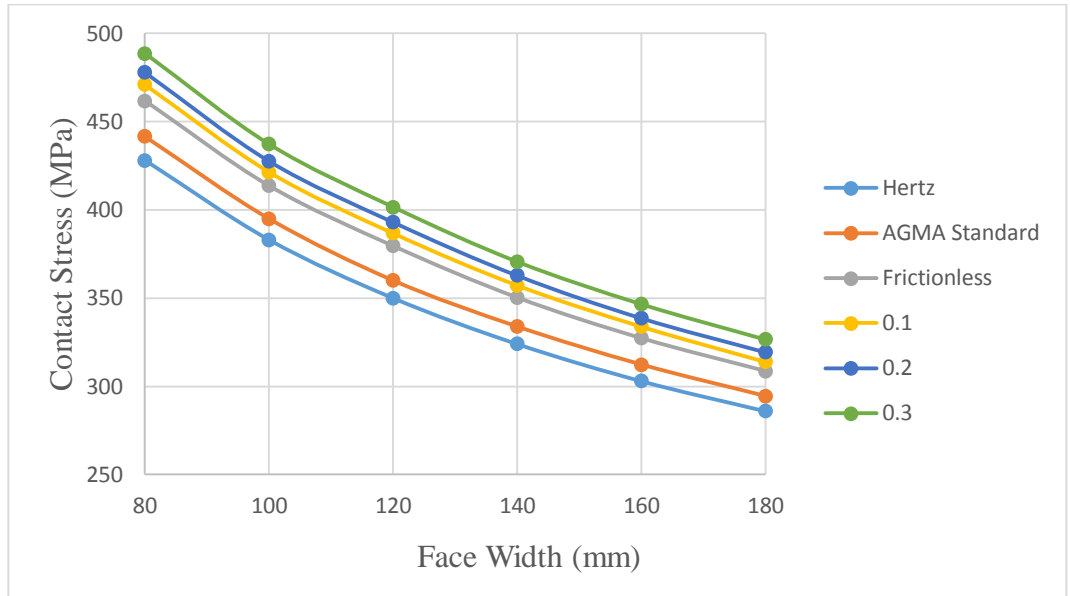


Figure 4.9: Contact Stress against Face Width under the Influence of Friction

Similar to analytical calculation graph, the FEA graph shows the typical result of contact stress against face width. Initially the author stated that load distribution along the face width was assumed to be uniform. The author's assumption is correct because along the face width, the contact stress distribution was uniformly distributed. The maximum contact stress was at the tip of the tooth. This is because when gear rotates, the tip of tooth is the first part to slide on the other tooth. Therefore, it is important to protect this part of teeth. Figure 4.10 shows the contact stress that occurs at the tip of a tooth.

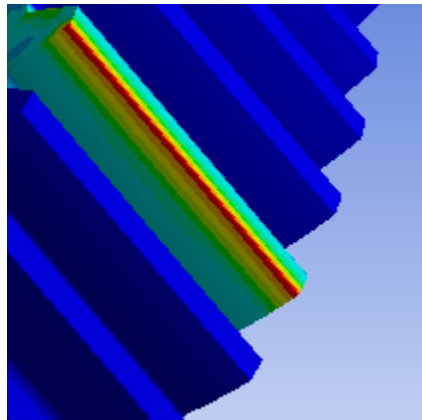


Figure 4.10: Contact Stress Distribution along the Tip of Tooth

CHAPTER 5

CONCLUSION AND RECOMMENDATION

As the conclusion, the objectives of this project which are to find the relationship between friction and contact stress have been achieved. As most previous researches in contact stress did not include the effect of friction, this study will be significant to the industry. This is because friction can determine the efficiency and performance of the gear, and thus need to be highly considered. It was found that the higher the friction, the higher the contact stress

The frictionless simulation showed that the finite element method is suitable to analyse the behaviour of contact stress in spur gear. This is shown by the amount of percentage error which is below 10%. Besides, ANSYS Workbench is suitable to solve frictional contact stress problem with its user friendly interface. From the simulation, an equation was defined that illustrates the relationship between contact stress and frictional coefficient. It was also found that the maximum contact stress will develop at the pitch contact between the teeth. Lastly, the maximum contact stress on the face width that has been influenced by friction is uniformly distributed.

However, the simulation alone is not enough to validate the result. The experimental approach also needs to be conducted [6]. This is because there are other factors that need to be considered such as quality of gear manufacture, the surface condition of the gear and many more.

REFERENCES

- [1] K.L. Johnson, Contact Mechanics, Cambridge University Press, 1985.
- [2] S. Cananau, "3D contact stress analysis for spur gear," National Tribology Conference, 2003, pp. 349-351
- [3] A.R. Hassan, "Contact stress analysis of spur gear tooth pair" in World Academy of Science, Engineering and Technology, 2009.
- [4] S.P. Shinde, A.A. Nikam, and T.S. Mulla, "Static analysis of spur gear using finite element analysis," IOSR Journal of Mechanical and Civil Engineering 2278-1684, pp. 23-31, 2010.
- [5] R. Gurumani, and S. Shanmugam, "Modeling and contact analysis of crowned spur gear teeth," *Engineering MECHANICS*, 1 (1), pp. 65-78, 2011.
- [6] R. Martins, R. Amaro, J. Seabra, "Influence of low friction coatings on the scuffing load capacity and efficiency of gears," *Tribology International*, vol. 41, (3), pp. 234-243, 2008.
- [7] A.I. Stefancu, S.C. Melenciuc, and M. Budescu, (2011). "Finite element analysis of frictional contacts," *Buletinul Institutului Politehnic Din Iasi*, vol. 8 (3), pp. 132-139, 2011.
- [8] S.C. Hwang, J.H. Lee, D.H. Lee, S.H. Han, and K.H. Lee "Contact stress analysis for a pair of mating gears." *Mathematics and Computer Modelling*, vol 57 (2), pp. 40-49, 2013.
- [9] S. Vijarangan, and N. Ganesan, "Static contact stress analysis of a spur gear tooth using the finite element method including frictional effects," *Computers and Structures*, vol 51 (6), pp. 765-770, 1994
- [10] J.R. Koisha, and H.P. Doshi, "Influence of friction on contact stress for small power transmission planetary gear box." *International Journal of Engineering Research and Development*, vol 1, 38-43, 2012.
- [11] R.R.G. Budynas, J.K. Nisbett, J.E. Shigley, Shigley's Mechanical Engineering Design, USA: McGraw-Hill Education, 2011.
- [12] S.S. Bhavikatti, Finite Element Analysis, New Delhi: New Age International Limited Publisher, 2005.
- [13] I.G. Perez, J.L. Iserte, and A. Fuentes, "Implementation of Hertz theory and validation of a finite element model for stress analysis of gear drives with localized bearing contact." *Mechanism and Machine Theory*, vol 46, pp. 765-783, 2011

- [14] Y.C. Hamand, and V. Kalamkar, "Analysis of stresses and deflection of sun gear by theoretical and ANSYS method." *Modern Mechanical Engineering*, vol 1, pp. 56-68, 2011.
- [15] C. Qi, Z. Han, and H. Kang, "Analysis of micro-segment gear's contact stress based on CATIA and ANSYS" in *International Conference on Digital Manufacturing & Automation*, (2010)
- [16] S.S. Rao, *Finite Element Method in Engineering*, Oxford: Butterworth-Heinemann, 2005.
- [17] O. Weck. and I.Y. Kim, "Finite element method. " Power Point presentation. Massachusetts Institute of Technology. 12 January 2004
- [18] S. Kumar, K.K. Mishra, and J. Madan, "Stress analysis of spur gear using FEM method" in *National Conference on Advancements and Futuristic Trends in Mechanical and Materials Engineering*, 2010
- [19] Y. Nakasone, *Engineering Analysis with ANSYS Software*, UK: Elsevier Butterworth-Heinemann, 2006.
- [20] D.W. Dudley, *Handbook of Practical Gear Design*, USA: CRC Press. 1994.
- [21] F.D. Jones and H.H. Ryffel, *Gear Design Simplified*, New York: Industrial Press INC. 1961.

APPENDICES

APPENDIX 3-1

FYP 1 GANTT CHART AND KEY MILESTONE

ACTIVITIES	Week													
	1	2	3	4	5	6	7	8	9	10	11	12	13	14
Phase I (Project Title Selection)														
FYP Briefing														
Meeting with Supervisor														
Preliminary Research Work														
Phase II (Project Proposal)														
Identification of Scope: Friction Contact Stress														
Submission of Extended Proposal														
Proposal Defence														
Phase III (Interim Report)														
Research on Analytical Hertz Equation														
Research on Friction														
ANSYS Tutorial														
Submission of Interim Report														

	Process
	Key Milestone

APPENDIX 3-2

FYP 2 GANTT CHART AND KEY MILESTONE

ACTIVITIES	Week													
	1	2	3	4	5	6	7	8	9	10	11	12	13	14
Phase I (Project Continuation)														
Analytical Calculation by using Hertz Theory														
Modelling of the gear														
Simulation by ANSYS														
Submission of Progress Report														
Project Continuation														
Phase II (Project Report)														
Pre-Sedex														
Submission of Draft Report														
Submission of Project Dissertation (Soft Bound)														
Submission of Technical Paper														
Oral Presentation														
Submission of Project Dissertation (Hardbound)														

	Process
	Key Milestone

APPENDIX 4-1

Full Results of Contact Stress against Load under the Influenced of Friction

Load (N)	Frictionless Contact Stress (MPa)	Contact Stress (MPa), $f=0.1$	Contact Stress (MPa), $f=0.2$	Contact Stress (MPa), $f=0.3$
1000	62.878	64.02	65.08	66.58
2000	105.36	107.2	109.05	111.53
3000	142.73	145.44	147.87	151.15
4000	180.41	184.008	186.72	190.87
5000	212.84	216.95	220.72	224.97
6000	258.22	262.61	267.00	273.50
7000	296.82	302.46	307.50	314.34
8000	339.66	347.12	355.55	359.37
9032	379.52	386.79	393.13	401.58
10000	415.92	423.82	430.89	439.63
11000	500.49	510.10	518.01	529.52
12000	515.30	524.58	535.10	545.21
13000	531.88	541.99	551.03	562.20

